Photocage Compounds

Deutsche Ausgabe: DOI: 10.1002/ange.201505778
Internationale Ausgabe: DOI: 10.1002/anie.201505778

A Zinc(II) Photocage Based on a Decarboxylation Metal Ion Release Mechanism for Investigating Homeostasis and Biological Signaling

*Prem N. Basa, Sagar Antala, Robert E. Dempski, and Shawn C. Burdette**

Abstract: *Metal ion signaling in biology has been studied extensively with ortho-nitrobenzyl photocages; however, the low quantum yields and other optical properties are not ideal for these applications. We describe the synthesis and characterization of NTAdeCage, the first member in a new class of Zn^{2+} photocages that utilizes a light-driven decarboxylation reaction in the metal ion release mechanism. NTAdeCage binds Zn^{2+} with sub-pM affinity using a modified nitrilotriacetate chelator and exhibits an almost 6 order of magnitude decrease in metal binding affinity upon uncaging. In contrast to other metal ion photocages, NTAdeCage and the corresponding Zn^{2+} complex undergo efficient photolysis with quantum yields approaching 30%. The ability of NTAdeCage to mediate the uptake of $^{65}Zn^{2+}$ by Xenopus laevis oocytes expressing hZIP4 demonstrates the viability of this photocaging strategy to execute biological assays.*

The importance of Zn^{2+} beyond structural and catalytic functions in proteins has become increasingly apparent.[1] Zinc and iron regulated proteins (ZIPs) increase cytosolic Zn^{2+} concentrations; in contrast, zinc transporter (ZnT) proteins decrease cytosolic Zn^{2+}.[2,3] Elucidating the function of free or loosely bound Zn^{2+} in the cytosol as well as in intracellular compartments remains important; however, the ability to modulate Zn^{2+} levels in vivo in a time-resolved manner remains elusive.[4] Free Zn^{2+} has been implicated in various signaling pathways,[1] and recently fertilization of oocytes has been shown to trigger "zinc sparks" that serve to initiate meiosis at the beginning stages of embryotic development.[5] The development of new methodologies to simulate fluctuations in Zn^{2+} concentrations in a spatiotemporal manner would facilitate the understanding of complex signaling processes.

The photochemistry of *ortho*-nitrobenzyl (*o*NB) chromophores initially was recognized as a means to deliver Ca^{2+} in a controlled manner to biological receptors using light.[6] We subsequently adapted two Ca^{2+}-releasing strategies to develop photocaged complexes for biologically relevant metal ions such as Zn^{2+}, Cu^{+} and Fe^{3+}.[7,8] In the *Cast* photocages, decreased electron density on a coordinated aniline nitrogen atom following photolysis lowers chelator binding affinity.[9–11] While this strategy can adequately buffer Ca^{2+} at typical intracellular resting levels (ca. 100 nM) and simulate biologically relevant concentration increases,[6,12] the reliance on weakly coordinating aniline-based ligands precludes use with Zn^{2+}, which experiences tighter intracellular homeostasis.[11] Alternatively, photolytically breaking a carbon-heteroatom bond provides compounds that release metal ions through the reduction of chelate effects. The *Cleav* class of photocaged complexes can effectively buffer and release Ca^{2+},[13] $Cu^{2+/1+}$,[14,15] or Zn^{2+} depending on the ligand design.[16,17]

Photocages based on *o*NB remain the dominant technology to study signal transduction mediated by biomolecules despite limitations like slow analyte-release kinetics, the requirement of UV light for photolysis and the formation of potentially toxic nitroso photoproducts.[18] In addition to these shortcomings, incorporating ligands into an *o*NB-scaffold can interfere with the uncaging mechanism. Both classes of photocaged complexes described above often exhibit low quantum yields (< 5%) owing to resonance between receptor donor atoms and the reactive *aci-nitro* intermediate generated by irradiating *o*NB chromophores.[19] Since *o*NB photochemistry inherently limits uncaging efficiency, we sought alternative strategies to design photocaged complexes that buffer Zn^{2+} at physiologically relevant levels and release the metal ion efficiently with high quantum yields.

Photodecarboxylation-based analyte releasing strategies recently have emerged as promising alternatives to *o*NBs.[20] Both ketoprofen and xanthone derived photocages exhibit ultrafast release kinetics, clean photochemistry, higher quantum yields and less toxic photoproducts than analogous *o*NB compounds.[21] Nitrophenylacetates (NPAs) utilize a similar photodecarboxylation mechanism, but require UV light to initiate the uncaging chemistry.[22–24] Although both *o*NB and NPAs contain nitrobenzyl groups, NPA decarboxylation does not involve the hydrogen atom abstraction utilized in *o*NB uncaging. Despite the potential advantages, this type of decarboxylation process has not been applied to metal ion photocages. A siderophore-inspired ligand to metal charge transfer process has been applied to photocage-like Fe^{3+} chelators;[25,26] however, this release strategy utilizes a photochemical mechanism that cannot be applied to redox-inactive metal ions like Zn^{2+}.

To test the hypothesis that Zn^{2+} could be released by decarboxylation, we envisioned a photocage integrating a nitrilotriacetate (NTA) receptor and a *meta*-NPA chromophore. Based on the mechanistic studies of photoactive *meta*-substituted compounds,[27,28] we expected the α-carbanion formed after the decarboxylation to be oxidized to an imine radical-anion (Scheme S1 in the Supporting Information).

[*] Dr. P. N. Basa, S. Antala, Prof. Dr. R. E. Dempski, Prof. Dr. S. C. Burdette
Department of Chemistry and Biochemistry
Worcester Polytechnic Institute
100 Institute Road, Worcester, MA 01609-2280 (USA)
E-mail: scburdette@wpu.edu

Supporting information for this article is available on the WWW under http://dx.doi.org/10.1002/anie.201505778.

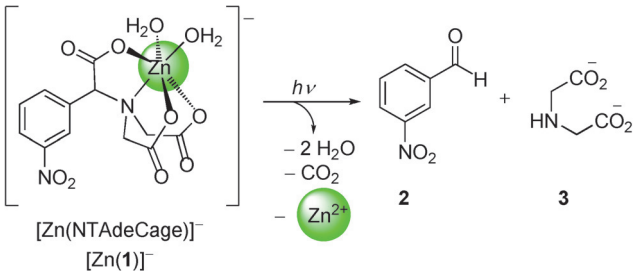

Figure 1. Uncaging action of [Zn(NTAdeCage)]$^-$. Photodecarboxylation followed by deamination produces both *m*-nitrobenzaldehyde and a more weakly Zn^{2+}-binding iminodiaceticacid (IDA) ligand. The NTAdeCage nomenclature refers to the nitrilotriacetate (NTA) chelator as well as the decarboxylation mechanism of the metal ion photocage.

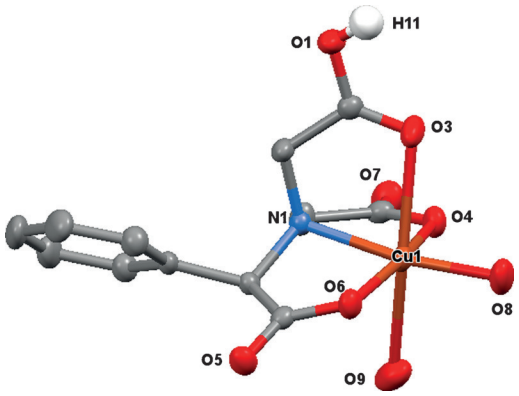

Figure 2. ORTEP diagram of [Cu(**6**)$(OH_2)_2$]·H_2O showing 50% thermal ellipsoids and selected atom labels. The unbound water molecule and the hydrogen atoms are omitted for clarity, except H11 that designates the protonated carboxylate ligand. The axial carboxylate carbonyl oxygen atom O3 and water oxygen atom O9 exhibit longer Cu bonds than the equatorial ligands owing to Jahn–Teller distortion.

Hydrolysis of the imine would then yield iminodiacetic acid (**3**, IDA) and *m*-nitrobenzaldehyde photoproducts (Figure 1). While uncaging NPAs requires UV irradiation, the wavelengths are comparable to those used for traditional *o*NB photocages. We reasoned that the metal ion would not directly interact with the photochemical intermediate unlike *o*NB, so the corresponding photocaged complex would retain the photophysical features of the parent compound. If the new metal ion releasing strategy proved successful, a new class of NPA-based photocages could be accessed, and the basic design strategy could be applied to other decarboxylation chromophores.

Unlike other potential decarboxylation systems, the NPA platform provides a readily accessible starting material and high yielding route to metal ion photocages. NTAdeCage (**1**, *NTA de*carboxylation photo*Cage*) can be prepared by converting L-phenyl glycine to the methyl ester (**4**, Scheme 1). Alkylation of amine with ethyl bromoacetate followed by saponification provides the desired triacid receptor (**6**). Site-specific nitration provides NTAdeCage in 78.5% yield from **6**. To elucidate the coordination chemistry of the modified NTA ligand, several metal salts and different crystal growing

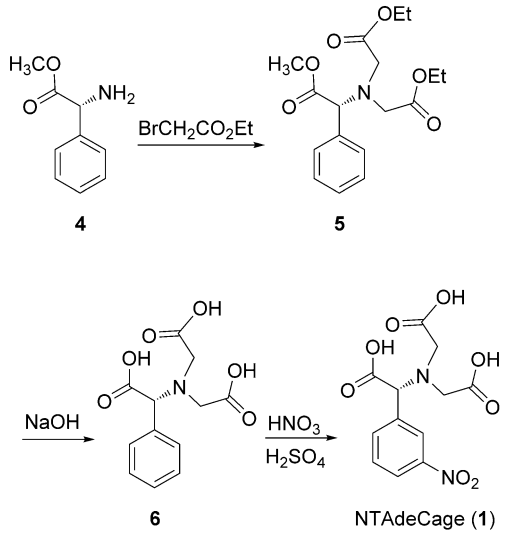

Scheme 1. Synthesis of NTAdeCage.

conditions were screened with **6**. While trials with Zn^{2+} failed to provide X-ray quality crystals, blue blocks of [Cu(**6**)$(OH_2)_2$]·H_2O complex were obtained by reacting the triacid ligand (**6**) with $CuCO_3$ (Figure 2). The complex adopts a classic Jahn–Teller distorted octahedral geometry, where one water ligand and a protonated carboxylate exhibit elongated metal–ligand bonds. The three equatorial Cu–O bond lengths of 1.963(9) Å, 1.957(6) Å, 1.972(7) Å, and the Cu–N bond length of 2.021(5) Å are significantly shorter than the axial Cu–O distances of 2.351(3) Å and 2.384(9) Å. Protonation of the axial carboxylate group leaves the complex with a net neutral charge. The coordination chemistry of [Zn(NTAdeCage)]$^-$ probably mimics that of an analogous octahedral [Zn(NTA)]$^-$ complex.[29] Although we typically generate [Zn(NTAdeCage)]$^-$ in situ for spectroscopic assays, the complex also can be isolated from the reaction of NTAdeCage and $Zn(OH)_2$. ^{1}H NMR analysis revealed an upfield shifting and splitting of methylene protons and the IR spectrum exhibited the characteristic carbonyl signals of zinc coordinated carboxylic groups. Furthermore HRMS confirmed the identity of the expected complex (*m*/*z* 374.98). NMR titration data is consistent with a 1:1 binding stoichiometric mode. While 2:1 $[Zn(NTA)_2]^{4-}$ complexes can form under certain conditions, the affinity data suggests the 1:1 complex will dominate in the absence of excess ligand.[30]

To assess the photoactivity of NTAdeCage and the corresponding metal complexes, the compounds were exposed to 365 nm light (3 W cm^{-2}) (Figure 3) and the photoreaction was analyzed by LCMS and GCMS. After irradiating a 1.12 mM solution of NTAdeCage (40 mM HEPES, 100 mM KCl, pH 7.5) a new peak appears in the LC trace that corresponds to a compound with *m*/*z* 151.0 (measured by GCMS) with a concomitant decrease in the LC peak corresponding to NTAdeCage (RF = 1.7, 254 nm, *m*/*z* 312.0). In the presence of 1 equiv of Zn^{2+}, the [Zn(NTAdeCage)]$^-$ complex (RF = 2.7, 254 nm, *m*/*z* 375.0) can be observed in the LC trace and an identical photoproduct peak can be found by GCMS after photolysis. Although the

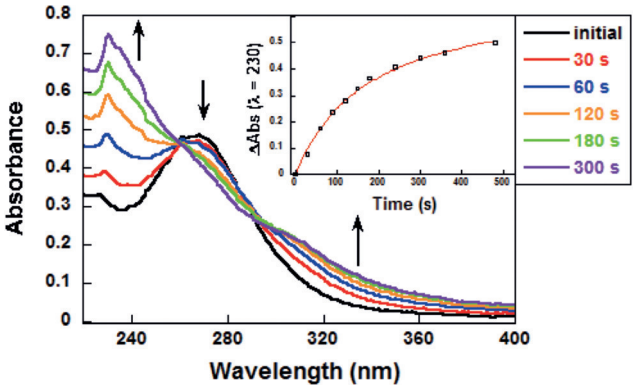

Figure 3. Photolysis of $[Zn(NTAdeCage)]^-$ (80 μM) under simulated physiological conditions (40 mM HEPES, 100 mM KCl, pH 7.5). Irradiation at 365 nm (LED, 3 Wcm^{-2}) leads to the erosion of the absorption band at 274 nm associated with the photocaged complex and the concurrent formation of a band at 230 nm characteristic of photoproduct **2**. Inset: change in absorbance at 230 nm with respect to photolysis time in seconds.

photoproduct appeared in the LC trace in both experiments, the *m*/*z* of photoproduct could not be detected by the coupled MS instrument, so the photolyzed sample was subjected to additional GCMS analysis. The mass of the photoproduct (*m*/*z* 151) and the fragmentation pattern (*m*/*z* 105.0, 77.1 and 51.0) match the theoretical and actual 3-nitrobenzaldehyde (**2**) spectrum. By monitoring the disappearance of NTAdeCage or the $[Zn(NTAdeCage)]^-$ complex, under these experimental conditions the quantum yields ($\Phi_{photolysis}$) were found to be $29 \pm 2\%$ and $27 \pm 5\%$ respectively.

In addition to the expected photoproducts (Figure 1), several minor photoproducts observed in the LCMS indicate the formation of α-amino radicals and possible coupling between nitro compounds and **2**; however, Zn^{2+}-binding appears to suppress these alternate photolysis pathways yielding cleaner conversion to **2** (Figure S3 and S4). A similar product distribution is observed when the photolysis is carried out in slightly basic water (pH 7.5) in the absence of buffer (Figure S1 and S2). Under non-aqueous conditions, such as in methanol, the relative amount of these minor photoproducts increases. Future detailed mechanistic studies will help identify ligand design factors that limit radical branching pathways and understand the uncaging mechanism in greater detail.

Multiple spectroscopic analyses of the photoreaction also confirm the LC/GCMS observations. The UV/Vis spectrum of 80 μM $[Zn(NTAdeCage)]^-$ (40 mM HEPES, 100 mM KCl, pH 7.5) contains an absorption band at 274 nm and a minor feature at 320 nm. During photolysis ($\lambda_{ex} = 365$ nm), the intensity of the 274 nm band decreases and a new peak forms at 230 nm with an isosbestic point at 254 nm that corresponds to the absorption of **2**. The increase in absorbance at 320 nm is attributed to the tail of the nitrobenzaldehyde peak and the formation of the minor photoproducts observed in the LCMS. Complete photolysis of NTAdeCage and the $[Zn(NTAdeCage)]^-$ complex occur within 6 min (Figure 3). When monitoring the photolysis by ^1H NMR spectroscopy, the aliphatic protons initially sharpen and then erode as a new peak appears at 10.1 ppm, corresponding to an aldehyde α-hydrogen of **2** (Figure S27). Furthermore, bulk photolysis provided **2** as the major product. The identity of this product was confirmed by TLC, NMR, FTIR, LC-MS and GC-MS analysis.

We employed established protocols using 4-(2-pyridylazo)resorcinol (PAR) to quantify metal binding properties of NTAdeCage since the Zn^{2+} complex lacks a spectroscopic signature.[17] The PAR signal changes fit a 1:1 Zn^{2+}:NTAdeCage binding model (Figure S9 and S10). Measurements in triplicate reveal a K_d of 0.10 ± 0.01 pM (40 mM HEPES, 100 mM KCl, pH 7.0). This value is comparable to that of unmodified NTA measured under the same conditions with PAR ($K_d = 3.7 \pm 0.4$ pM) and the values measured by potentiometric titration ($\log K = 10.7$, $K_d = 19.9$ pM).[31] The IDA photoproduct has log *K* of 7.2 for Zn^{2+} at pH 7 ($K_d =$ 63 nM),[31] so the ΔK_d (K_d IDA/K_d NTAdeCage) for this photocaging system is nearly 630 000. The ΔK_d value provides a convenient means to compare the metal ion releasing properties of different photocages semi-quantitatively. The ΔK_d of NTAdeCage is smaller than those measured for *Cleav* photocages, but is significantly higher than any *Cast* photocage measured to date.[7]

We also used a metal ion displacement assay to evaluate the impact of the other biologically relevant divalent cations on the photocaged complex. By titrating $[Zn(NTAdeCage)]^-$ with Ca^{2+} or Mg^{2+} in the presence of PAR, the appearance of the $[Zn(PAR)_2]$ can be used to ascertain the concentration at which interference becomes problematic. While no displacement was observed from $[Zn(NTAdeCage)]^-$ when titrating with Mg^{2+}, at approximately 100 μM, a 10-fold excess with respect to $[Zn(NTAdeCage)]^-$ in the selectivity experiment, Ca^{2+} displaces most of the bound Zn^{2+} yielding $[Ca(NTAdeCage)]^-$ (Figure S13); however, at typical resting intracellular $[Ca^{2+}]$ (ca. 100 nM), the displacement is negligible. Provided Ca^{2+} do not exceed normal basal levels, $[Zn(NTAdeCage)]^-$ should deliver Zn^{2+} as desired upon photolysis.

Both the buffering capacity NTAdeCage prior to irradiation and the magnitude of the ΔK_d after photolysis indicate the photocage should be suitable for biological applications where resting free Zn^{2+} concentrations are in the nM range. To demonstrate metal ion release, $[Zn(NTAdeCage)]^-$ was photolyzed and ZTRS,[32] a fluorescent Zn^{2+} sensor ($K_d =$ 5.7 nM) was used to monitor increases in available Zn^{2+} (Figure S11 and S12). Aliquots from a bulk $[Zn(NTAdeCage)]^-$ solution being photolyzed were analyzed owing to ZTRS photobleaching that occurred when the sensor was exposed to the light source for uncaging. An increase in fluorescence intensity at 512 nm, which is consistent with emission of $[Zn(ZTRS)]^{2+}$, in aliquots from the photolyzed $[Zn(NTAdeCage)]^-$ solutions treated with ZTRS, demonstrates that while higher affinity NTAdeCage chelator effectively competes with ZTRS for Zn^{2+}, the IDA photoproduct does not. The composite spectroscopic investigations and proof-of-concept Zn^{2+} releasing assays demonstrate the validity of the proposed uncaging mechanism.

The feasibility for using this photocage in biological systems was demonstrated by measuring Zn^{2+} transport following the heterologous expression of the human (h) zinc

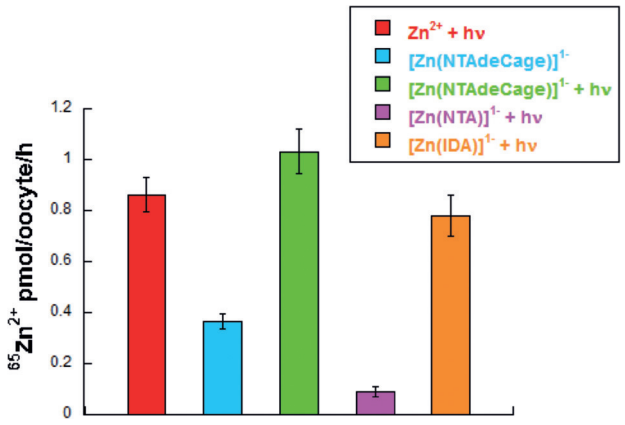

Figure 4. $^{65}Zn^{2+}$ uptake in oocytes expressing hZIP4. Oocytes were subjected to $^{65}Zn^{2+}$ by incubating them with 250 nM $^{65}ZnCl_2$ or 250 nM $^{65}ZnCl_2$ in the presence of 250 μM of NTAdeCage, NTA or IDA. All oocytes except the $[Zn(NTAdeCage)]^-$ control set were exposed to 3 min of 365 nm light (LED, 3 Wcm^{-2}). The assay was performed as described previously.[33] Each bar represents the data from the analysis of 9 to 12 oocytes. The uptake values shown are the mean values with standard error.

transporter ZIP4 in *Xenopus laevis* oocytes. The oocyte expression system is a robust medium to examine the kinetics, specificity and mechanism of hZIP4.[33] In this experiment (Figure 4), we incubated oocytes expressing hZIP4 or water-injected controls with 250 nM $^{65}ZnCl_2$, $[^{65}Zn(NTAdeCage)]^-$ in the absence of light, $[^{65}Zn(NTAdeCage)]^-$ exposed to light, $[^{65}Zn(NTA)]^-$ exposed to light, or $^{65}Zn(IDA)]^-$ exposed to light. For these experiments, water-injected oocytes were subtracted from mRNA-injected oocytes. Under these experimental conditions, free $^{65}Zn^{2+}$, uncaged $^{65}Zn^{2+}$ (by light from NTAdeCage) or $^{65}Zn^{2+}$ in the presence of the photocage product (IDA) had transport rates which were similar. In contrast, $^{65}Zn^{2+}$ coordinated to NTA or $^{65}Zn^{2+}$ coordinated to the photocaged complex in the absence of light were transported by hZIP4 at a lower rate. The results suggest that both tetradentate chelators bind $^{65}Zn^{2+}$ tightly, which inhibits transport by hZIP4. Upon photolysis of $[^{65}Zn(NTAdeCage)]^-$, $^{65}Zn^{2+}$ becomes available for uptake by hZIP4. The slight increase in uptake between $[^{65}Zn(NTAdeCage)]^-$ in the absence of light and light-exposed $[^{65}Zn(NTA)]^-$ may be due to a ligand exchange process with the transporter that becomes more favorable due to hydrophobic interactions between the photocage aryl group and the oocyte membrane or hZIP4.

In summary, we have devised a new strategy to release metal ions from a chelating ligand using a photodecarboxylation reaction. NTAdeCage binds Zn^{2+} with sub-pM affinity and exhibits a reduction in metal binding affinity after efficient uncaging with 365 nm light. The quantum yields of uncaging represent a greater than 5-fold improvement over Zn^{2+} photocages containing an *o*NB uncaging group. We have applied NTAdeCage to a Zn^{2+} uptake assay with hZIP4, which demonstrates this photocage can be applied to biological studies. We are currently interested in developing this photodecarboxylation strategy further by using both NPA and other chromophores to design Zn^{2+} photocaged complexes with improved photophysical and enhanced metal binding affinity and selectivity. In addition, we are developing protocols to expand the scope of biological assays that can be conducted with NTAdeCage.

Acknowledgements

We thank Prof. Peter Wan for guidance with photochemical mechanism proposals. This work was supported by NSF Grant CHE-0955361 and NIH grant GM105964.

Keywords: cage compounds · coordination compounds · photolysis · X-ray diffraction · zinc

How to cite: *Angew. Chem. Int. Ed.* **2015**, *54*, 13027–13031
Angew. Chem. **2015**, *127*, 13219–13223

[1] T. Fukada, S. Yamasaki, K. Nishida, M. Murakami, T. Hirano, *J. Biol. Inorg. Chem.* **2011**, *16*, 1123.
[2] R. E. Dempski, *Curr. Top. Membr.* **2012**, *69*, 221.
[3] M. Schweigel-Röntgen, *Curr. Top. Membr.* **2014**, *73*, 321.
[4] M. L. Bernhardt, B. Y. Kong, A. M. Kim, T. V. O'Halloran, T. K. Woodruff, *Biol. Reprod.* **2012**, *86*, 114.
[5] E. L. Que, R. Bleher, F. E. Duncan, B. Y. Kong, S. C. Gleber, S. Vogt, S. Chen, S. A. Garwin, A. R. Bayer, V. P. Dravid, T. K. Woodruff, T. V. O'Halloran, *Nat. Chem.* **2015**, *7*, 130.
[6] G. C. Ellis-Davies, *Chem. Rev.* **2008**, *108*, 1603.
[7] C. Gwizdala, S. C. Burdette, *Curr. Opin. Chem. Biol.* **2013**, *17*, 137.
[8] H. W. Mbatia, S. C. Burdette, *Biochemistry* **2012**, *51*, 7212.
[9] C. Gwizdala, P. N. Basa, J. C. MacDonald, S. C. Burdette, *Inorg. Chem.* **2013**, *52*, 8483.
[10] C. Gwizdala, D. P. Kennedy, S. C. Burdette, *Chem. Commun.* **2009**, 6967.
[11] C. Gwizdala, C. V. Singh, T. R. Friss, J. C. MacDonald, S. C. Burdette, *Dalton Trans.* **2012**, *41*, 8162.
[12] S. R. Adams, R. Y. Tsien, *Annu. Rev. Physiol.* **1993**, *55*, 755.
[13] G. C. Ellis-Davies, R. J. Barsotti, *Cell Calcium* **2006**, *39*, 75.
[14] K. L. Ciesienski, K. L. Haas, K. J. Franz, *Dalton Trans.* **2010**, *39*, 9538.
[15] H. W. Mbatia, H. D. Bandara, S. C. Burdette, *Chem. Commun.* **2012**, *48*, 5331.
[16] H. Bandara, T. P. Walsh, S. C. Burdette, *Chem. Eur. J.* **2011**, *17*, 3932.
[17] H. D. Bandara, D. P. Kennedy, E. Akin, C. D. Incarvito, S. C. Burdette, *Inorg. Chem.* **2009**, *48*, 8445.
[18] C. Brieke, F. Rohrbach, A. Gottschalk, G. Mayer, A. Heckel, *Angew. Chem. Int. Ed.* **2012**, *51*, 8446; *Angew. Chem.* **2012**, *124*, 8572.
[19] D. P. Kennedy, D. C. Brown, S. C. Burdette, *Org. Lett.* **2010**, *12*, 4486.
[20] G. Cosa, M. Lukeman, J. Scaiano, *Acc. Chem. Res.* **2009**, *42*, 599.
[21] J. A. Blake, M. Lukeman, J. C. Scaiano, *J. Am. Chem. Soc.* **2009**, *131*, 4127.
[22] K. Lommel, G. Schäfer, K. Grenader, C. Ruland, A. Terfort, W. Mäntele, G. Wille, *ChemBioChem* **2013**, *14*, 372.
[23] J.-M. Mewes, E. Pepler, J. Wachtveitl, A. Dreuw, *J. Phys. Chem. A* **2012**, *116*, 11846.
[24] J. D. Margerum, C. T. Petrusis, *J. Am. Chem. Soc.* **1969**, *91*, 2467.
[25] J. E. Grabo, M. A. Chrisman, L. M. Webb, M. J. Baldwin, *Inorg. Chem.* **2014**, *53*, 5781.
[26] H. Sayre, K. Milos, M. J. Goldcamp, C. A. Schroll, J. A. Krause, M. J. Baldwin, *Inorg. Chem.* **2010**, *49*, 4433.

[27] L. A. Huck, M. Xu, K. Forest, P. Wan, *Can. J. Chem.* **2004**, *82*, 1760.
[28] P. Wan, K. Yates, *Can. J. Chem.* **1986**, *64*, 2076.
[29] J. Oliver, B. Barnett, L. Strickland, *Acta Crystallogr. Sect. B* **1984**, *40*, 377.
[30] D. L. Rabenstein, R. J. Kula, *J. Am. Chem. Soc.* **1969**, *91*, 2492.
[31] A. E. Martell, R. J. Motekaitis, *Determination and Use of Stability Constants*, 2nd ed., Wiley, USA, **1992**.
[32] Z. Xu, K.-H. Baek, H. N. Kim, J. Cui, X. Qian, D. R. Spring, I. Shin, J. Yoon, *J. Am. Chem. Soc.* **2010**, *132*, 601.
[33] S. Antala, R. E. Dempski, *Biochemistry* **2012**, *51*, 963.

Received: June 23, 2015
Revised: July 29, 2015
Published online: September 8, 2015

